Article

Design and Control of an Acetic Acid Dehydration Column with *p*-Xylene or *m*-Xylene Feed Impurity. 2. Bifurcation Analysis and Control

Hao-Yeh Lee, and Hsiao-Ping HuangI-Lung Chien

Ind. Eng. Chem. Res., **2008**, 47 (9), 3046-3059 • DOI: 10.1021/ie070916f

Design and Control of an Acetic Acid Dehydration Column with *p*-Xylene or *m*-Xylene Feed Impurity. 2. Bifurcation Analysis and Control

Hao-Yeh Lee and Hsiao-Ping Huang*

Department of Chemical Engineering, National Taiwan University, Taipei 10617, Taiwan

I-Lung Chien

Department of Chemical Engineering, National Taiwan University of Science and Technology, Taipei 10672, Taiwan

In the production of terephthalic acid and isophthalic acid, a tiny amount of one reactant *p*-xylene or *m*-xylene may exist in the unreacted acetic acid, which needs to be purified for reuse by a dehydration column. In our previous study (Huang et al.[1]), it was found that the feed tray location is extremely important for optimizing the operating and the total annual costs. In this paper, the optimal designed processes with and without feed impurity will be further studied in terms of their bifurcation behavior and control. Three cases (one without feed impurity, one with feed impurity and side stream, and one with feed impurity but without side stream) will be studied. In this study, bifurcations due to output multiplicity are observed in two of the cases which have feed impurity but not in the case without. In each bifurcation case, the optimal base case is located on an unstable branch. The overall control at this unstable operating point is thus proposed to deal with disturbance from throughput or feed composition (e.g., water or the impurity) variations. It is found that a dual-temperature control scheme is necessary to keep products at both ends of the column within specifications. For the impurity disturbances, the side streamflow rate needs to be manipulated accordingly. A novel side-stream operating strategy to maintain the impurity concentration inside the column is proposed for an energy-efficient operation.

1. Introduction

Acetic acid (HAc) dehydration is an important operation in the production of terephthalic acid and isophthalic acid (Hindmarsh et al.[2] and Lee et al.[3]) or in the manufacture of cellulose acetate. To make the dehydration easier, an entrainer is often introduced into the system. In a review paper, Othmer[4] described an azeotropic distillation system containing a dehydrating column, a decanter, and a water column for the separation of HAc and water. In a paper by Pham and Doherty,[5] examples of using ethyl acetate (Tanake and Yamada[6]), *n*-propyl acetate (Othmer[7]), or *n*-butyl acetate as entrainers were listed in a table of examples of heterogeneous azeotropic separations. Siirola[8] uses HAc dehydration as an example to demonstrate a systematic design technique for synthesizing the process flowsheet. Ethyl acetate was used as the entrainer in that paper to design a complete HAc dehydration process using multiple-effect azeotropic distillation and heat integration. Wasylkiewicz et al.[9] proposed using a geometric method for the optimum design of an HAc dehydrating column with *n*-butyl acetate as the entrainer. Chien et al.[10] studied the design and control of an HAc dehydration system via heterogeneous azeotropic distillation. Isobutyl acetate (IBA) was selected from three candidate acetates as a suitable entrainer on the basis of the total annual cost (TAC) analysis. In that heterogeneous distillation column, only three components (HAc, H_2O, and the entrainer) were considered. In practical situations, HAc dehydration may be more complicated. For example, in the production of aromatic acids such as terephthalic and isophthalic acids by oxidizing *p*-xylene (PX) or *m*-xylene (MX), a slurry of terephthalic acid or isophthalic acid in the solvent HAc is produced. After separation of the product from the HAc and removal of H_2O by evaporation, the solvent HAc will be returned to the oxidation step (Hindmarsh et al.[2] and Lee et al.[3]). To recover the solvent HAc, a HAc dehydrating column is necessary. However, in this recovering step, tiny amounts of one reactant may also enter along with this aqueous HAc into the dehydration column.

For the feed of aqueous HAc containing an impurity for dehydration, Chien et al.[11] studied the design and operation of the process which has five feed streams. The entrainer used for this industrial column is also the IBA. In that paper, optimal side-stream location and its flow rate were designed, and an automatic purging strategy was proposed to prevent accumulation of an impurity (not specified for proprietary reasons) inside the column. However, the effect of the feed tray location was not investigated in that paper.

In one of our latest papers, dehydration columns via heterogeneous azeotropic distillation (Huang et al.[1]), with and without the tiny amounts of impurity in the feed stream, are considered for optimal design. Simulation results show that, without changing the feed location, an addition of 0.1 mol % of *p*-xylene or *m*-xylene into the feed stream will bring forth drastic differences in the optimized results. Over 50% more TAC and operating energy are needed to operate this column with side stream. However, by considering the feed tray location as an additional design variable in the optimization search, significant savings in TAC with a reduction of more than 21% can be realized. Note particularly with this change of the feed tray location significant saving of the reboiler duty with a reduction of more than 18% can also be achieved.

Besides the drastic change is the TAC, the existence of a tiny amount of impurities also has a remarkable effect on the control of this dehydration column. In this paper, the bifurcation

* To whom correspondence should be addressed. Tel: 886-2-2363-8999. Fax: 886-2-2362-3935. E-mail: huanghpc@ntu.edu.tw.

10.1021/ie070916f CCC: $40.75
Published on Web 04/02/2008

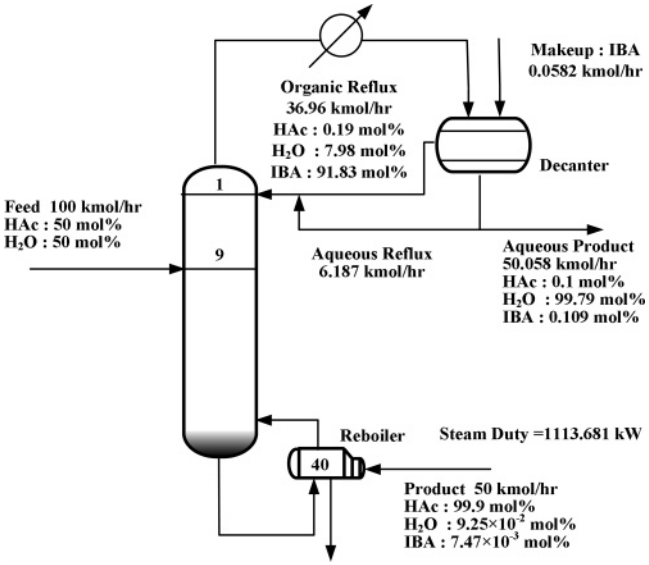

Figure 1. Process flowsheet for the case without feed impurity.

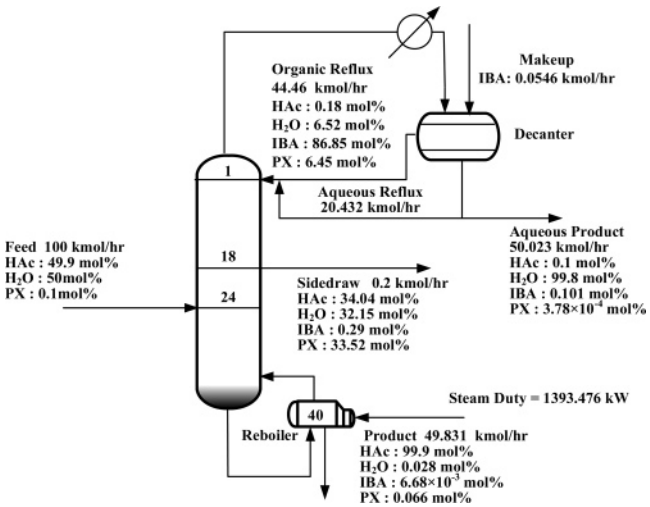

Figure 2. Process flowsheet for the case with feed impurity.

and dynamic analysis of three cases (one without feed impurity, one with feed impurity and side stream, and one with feed impurity but without side stream) will be investigated. The overall control strategy for the acetic acid dehydration process with side stream will be proposed. Only control of tray temperature will be used for product purity. The purpose of the overall control strategy is to maintain product purity despite feed flow rate or feed composition disturbances. For the feed impurity disturbances, the proper manipulation of the side streamflow will also be studied in order to ensure energy-efficient operation.

2. Process Flowsheets with and without Feed Impurity

In this HAC dehydration process, the HAC specifications are 99.9 mol % in the bottom and 0.1 mol % in the aqueous outlet from the decanter. In the case "without impurity", the feed stream is assumed to contain equal moles of HAc and H_2O and the IBA is introduced into the column through the organic reflux stream. The resulting optimal process flowsheet is given in Figure 1. The optimal flowsheet was found to have 40 total stages (including reboiler) with feed tray locating at the ninth stage and a fraction of aqueous reflux equaling to 0.11.

If a tiny PX or MX impurity exists in the feed stream, taking PX impurity as an example, the feed consists of 49.9 mol % HAc, 50 mol % H_2O, and 0.1 mol % PX. The base case result is very different from the above one that is free of impurity. In this "with impurity" case, the feed location moves to the 24th stage and a side stream at the 18th stage is required, to minimize TAC and the operating energy. The resulting flowsheet is summarized in Figure 2. Later on, a feed stream with PX impurity will be considered for dynamic analysis and control study. The process flowsheet with MX as impurity exhibits dynamic and control behavior very similar to the PX case; thus, the result for the MX case is omitted in this paper.

2.1. Multiple Steady-States Phenomena. In both the "without impurity" and "with impurity" systems, there are two manipulated variables adjustable to make products meet the top and bottom specifications. One is the aqueous reflux flow rate, and the other is reboiler duty. To investigate the open-loop stability of the optimal operating point for each case, manipulation variables perturbed by square pulse (i.e., 1 h width and ±1% high) one at a time are introduced at the 10th hour from the time origin. Notice, in these two cases, the top and bottom HAc compositions are considered as process variables.

For the "without impurity" case, the process variables respond to the pulse disturbance and return to its original steady state in 100 h. Figure 3 displays the results in time domain. As can be seen from the result, the steady state of the optimal operating point is stable.

On the other hand, in the "with impurity"case, the results are significantly different. After perturbed in either direction, the final steady state drifts away from its original steady state. From Figure 4, a positive pulse in aqueous reflux flow rate leads the column to reach another steady state after 1000 h, where $x_{B,HAc} = 99.57$ mol % and $x_{D,HAc} = 0.04356$ mol %. Conversely, perturbed in an opposite direction, the phase-splitting behavior in the decanter disappeared and the column operation collapsed after 104.8 h. Similar behavior appears if the process is perturbed by a square pulse with reboiler duty. The dynamic effect is even faster. With a pulse to reboiler duty in negative direction, the column top and bottom compositions reach a new steady state. However, a positive pulse in the reboiler duty will force the phase-splitting behavior in the decanter to disappear after 67.5 h and the column operation collapsed. In other words, under the above pulse input tests, the column discloses that to each set of input variables there are two steady states in correspondence. This phenomenon is known as output multiplicity or multiple steady states. The occurrence of multiple steady states only exists for "with impurity" case. No multiple steady states were found in the "without impurity" case.

2.2. Bifurcation Branches Analysis. To explore this multiple steady-state phenomenon further, the bifurcation branches of this system will be studied. The bifurcation branch is a trace of the steady states along a varying bifurcation variable which is one of the manipulation variables in this case. Figure 5 shows the bifurcation branches for the "with PX impurity" case. In each plot of this figure, the upper part gives the steady-state HAc composition in the bottom; the lower part gives the steady-state HAc composition at the top. The dashed line shown in the figure is the unstable bifurcation branch, and the solid line is the stable one. From this figure, it is found that when the aqueous reflux flow rate is less than 20.26 kmol/h, under a given reboiler duty of 1393.46 kW, the system would be unstable and none of the steady state can be found. Figure 5 also shows similar phenomenon while the reboiler duty is the bifurcation variable and greater than 1397.47 kW, under a constant reflux flow rate at 20.46 kmol/h.

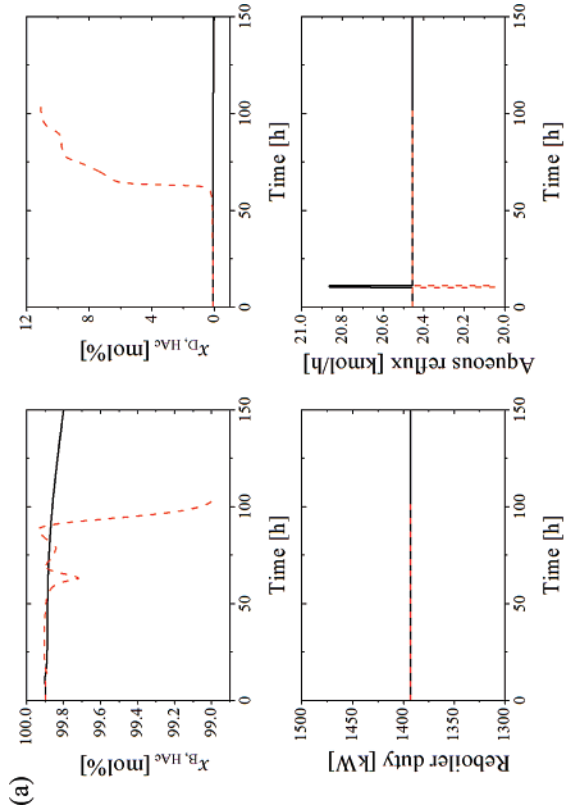

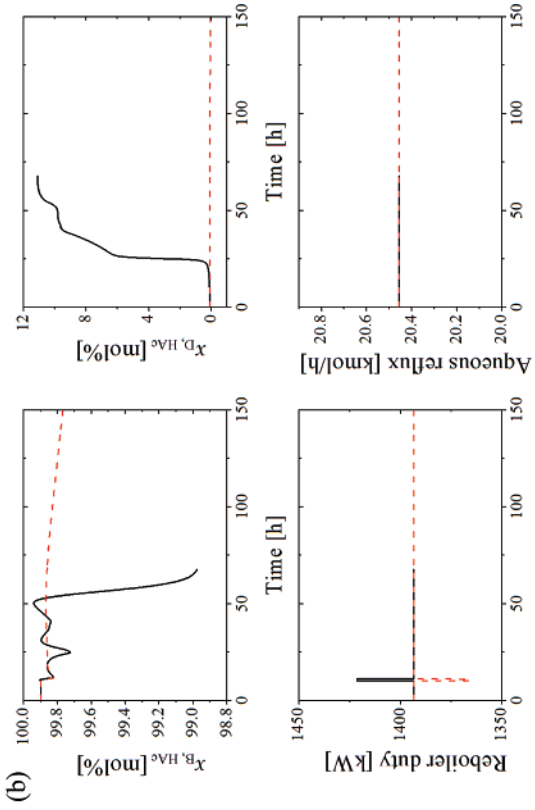

Figure 4. Square pulse responses for the process with feed impurity: (a) aqueous reflux change; (b) reboiler duty change.

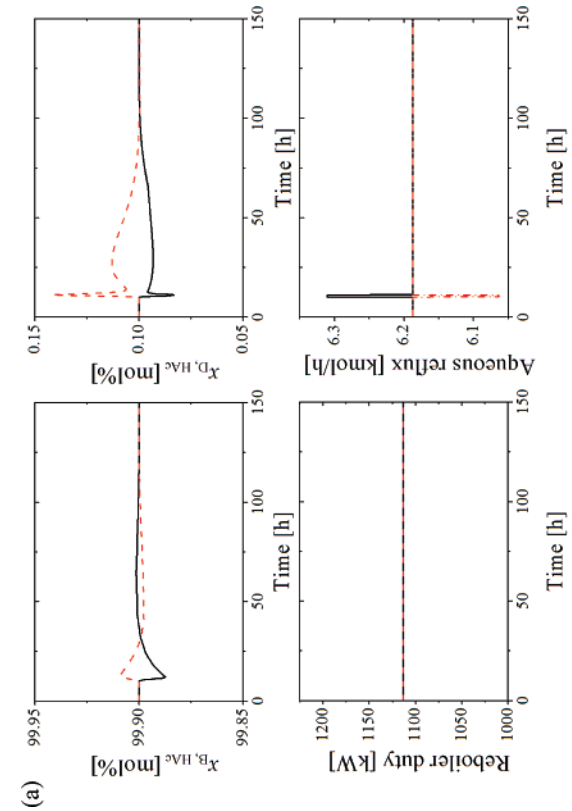

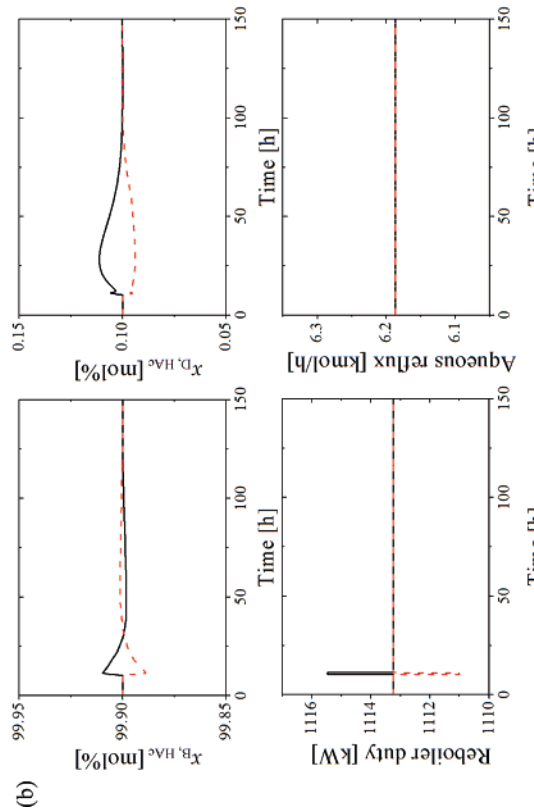

Figure 3. Square pulse responses for the process without feed impurity: (a) aqueous reflux change; (b) reboiler duty change.

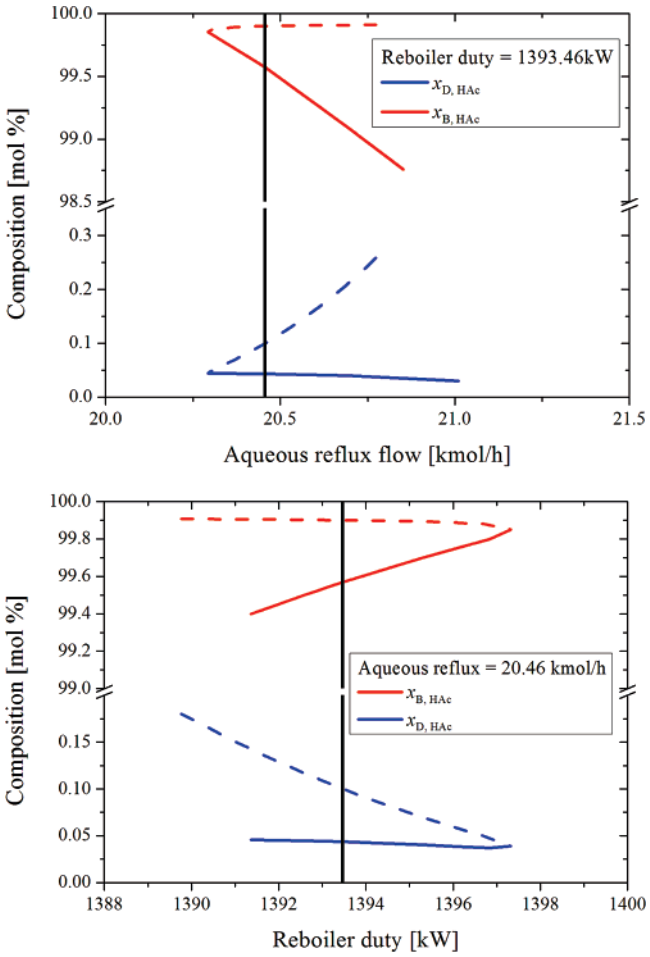

Figure 5. Bifurcation plot using aqueous reflux or reboiler duty as the bifurcation parameter.

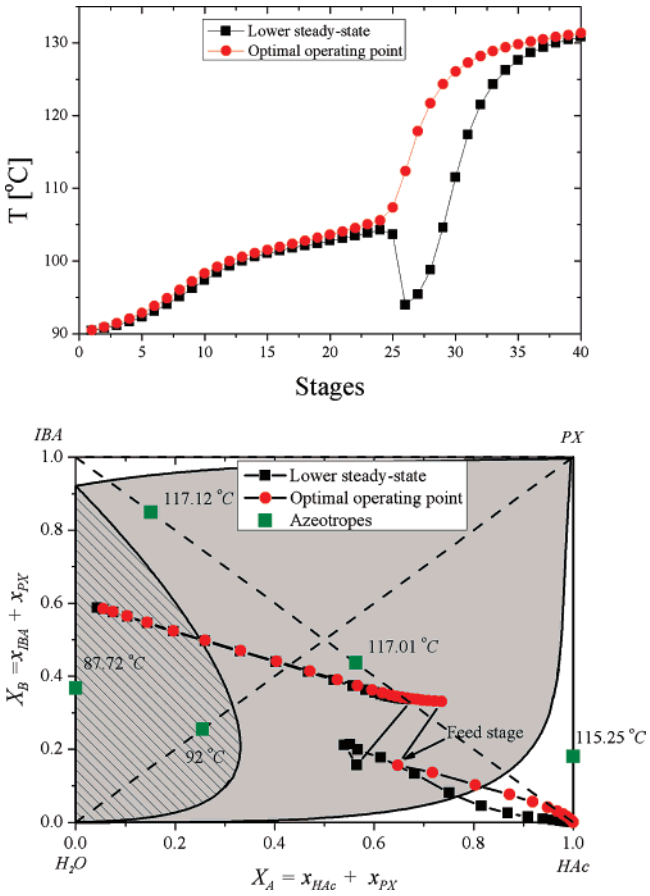

Figure 6. Temperature and composition profiles for optimal operating point and lower steady state.

From Figure 5, the points of bifurcation branches that cross vertical solid line are the optimal operating point ($x_{D,HAc}$, $x_{B,HAc}$) at (0.1 mol %, 99.9 mol %) and the lower stable steady-state point ($x_D{}^L{}_{,HAc}$, $x_B{}^L{}_{,HAc}$) at (0.04356 mol %, 99.57 mol %), under the same set of manipulating variable values. From the figure, the steady-state HAc compositions of the top and bottom will be either on the stable or on the unstable branch simultaneously. For example, the top and bottom HAc compositions of optimal operating point are both on the unstable branch and the compositions of the lower steady state are both on the stable branch.

Figure 6 shows the temperature and composition profiles for the optimal operating point and the lower steady state. For the composition profiles, Cruickshank et al.[12] orthogonal projection for four-component systems as used in our part 1 paper (Huang et al.[1]) are shown. From Figure 6a, it shows that the temperature profiles split obviously after the 24th stage (i.e., the feed location). For the optimal operating point, the temperature is monotonically increasing from column top to bottom. However, for the lower steady state, the temperature starts to drop down at the 25th stage and has the largest drop at the 26th stage. The composition profiles, as shown in Figure 6b, also show drastic changes below the feed location. The lower steady state follows the path with less PX in the lower part of the column.

3. Effect of Product Purity Specifications. The design to meet a lower HAc composition (99.5 mol %) specification at the bottom is considered in this section, where there is no need to include the side stream in the flowsheet. For this lower

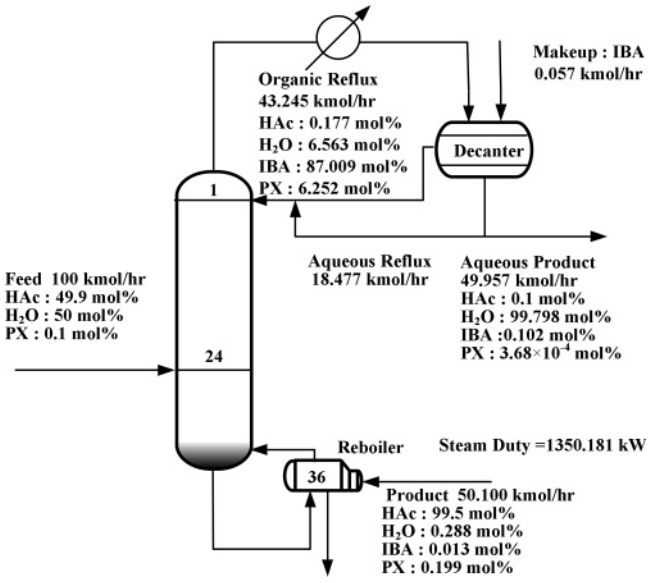

Figure 7. Optimal design flowsheet for the lower product purity case.

product purity specification, the specification of the top HAc composition is still set at 0.1 mol % HAc. The optimal design flowsheet for this lower product purity case was developed in Huang et al.[1] and is shown in Figure 7.

Following the analysis method in section 2, the multiple steady states were also found for this lower purity specifications system. There are also two bifurcation branches for each manipulated variable. Figure 8 shows the optimal operating point

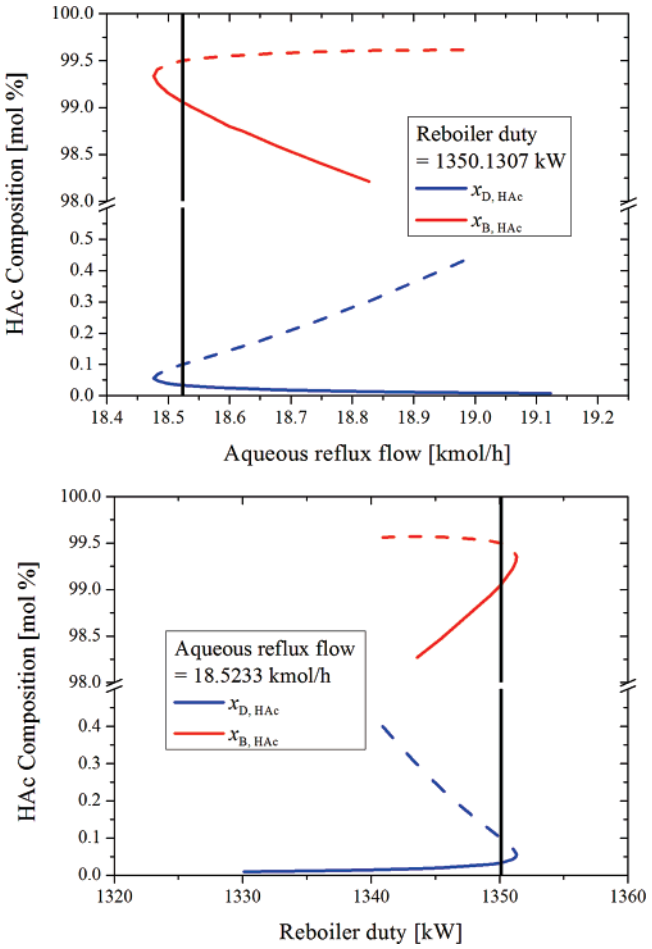

Figure 8. Bifurcation plot for the process with lower product purity specification.

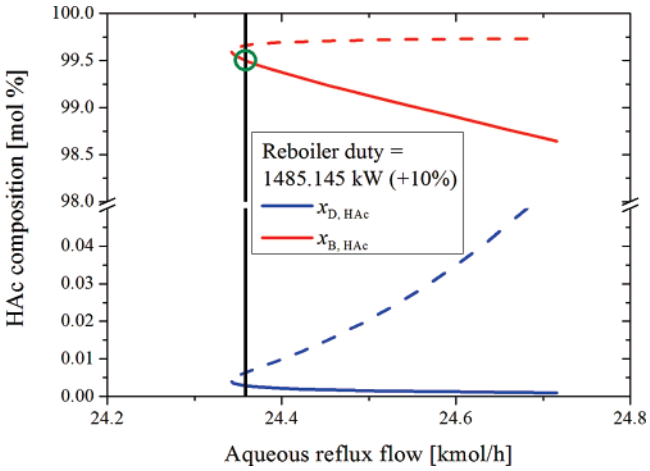

Figure 9. Effect of increasing reboiler duty for the process with lower product purity specification.

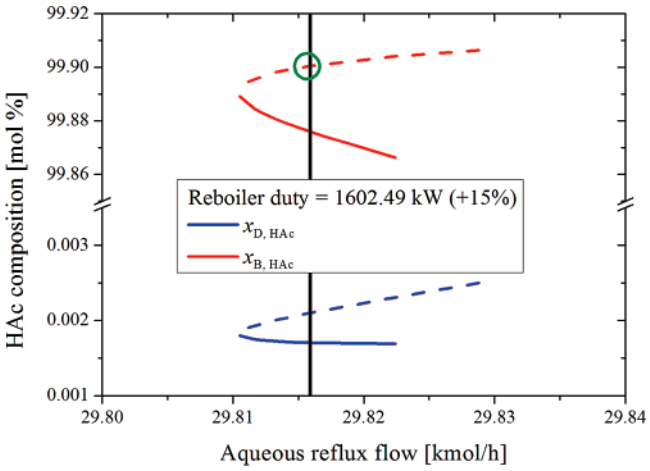

Figure 10. Effect of increasing reboiler duty for the process with higher product purity specification.

is also open-loop unstable. The HAc compositions will decrease from this unstable steady state to stable steady state ($x_{B,HAc}$ from 99.5 mol % to 99.06 mol % and $x_{D,HAc}$ from 0.1 mol % to 0.03355 mol %). The shapes of bifurcation branches are similar with higher and lower purity specifications (Figure 5 vs Figure 8). The only difference in the case with lower specifications is that the curve is smoother near the turning point. The above results represent that no matter if side stream exists or not, the bifurcation phenomenon occurs when the feed stream contains PX impurity.

For the controller design convenience, the operating point is preferable to move to a stable steady state. However, the process specifications cannot be achieved at the lower stable steady states because of too low of a bottom HAc composition. To solve this problem, a conservative condition by increasing reboiler duty is considered. Figure 9 displays that the system with lower purity specification needs about a +10% reboiler duty increase to move the operating point from an unstable steady state to a stable one, with the same bottom product specification. Similarly, the system with higher purity specification (99.9 mol % case) needs to increase more reboiler duty to move the steady state onto the stable branch. Nevertheless, as Figure 10 shows, even though the reboiler duty is increased up to +15%, the steady state is still on the unstable branch. As the results shown, there is a trade-off between TAC and easiness of controller design. It costs much more reboiler duty to operate the column at a stable steady state, especially for the case with higher purity specification. In the following, we will show how to control this column at the more economical unstable steady state. The system with higher purity specification (flowsheet as in Figure 2) will be used for the investigation of the control study.

4. Control Strategy Development. Basic inventory control loops are determined by first following the control strategy in Chien et al.[10] They are the following: column bottom level is controlled by manipulating the bottom flow; organic level is controlled by manipulating the organic reflux flow; aqueous level is controlled by manipulating the aqueous outlet flow; column top pressure is controlled by manipulating the top vapor flow. The remaining two important manipulated variables for product quality control are aqueous reflux flow and reboiler duty.

4.1. Temperature Control Strategy. In Chien et al.,[10] only a single temperature control loop is needed to hold the top and bottom products at their purity specifications by manipulating the aqueous reflux flow. The reboiler duty is fixed and maintains at a constant ratio to the fresh feed flow rate. However, their case is different from ours because there is no feed impurity presented in the system. Table 1 shows the results of our case in Figure 2 where the aqueous reflux flow and the reboiler duty are manipulated by two composition control loops when subjected to various disturbances. Of course, this situation is not feasible in industry because of the unavailability of on-line composition measurements. However, the results of these closed-loop runs can be considered as the targeting goal for the

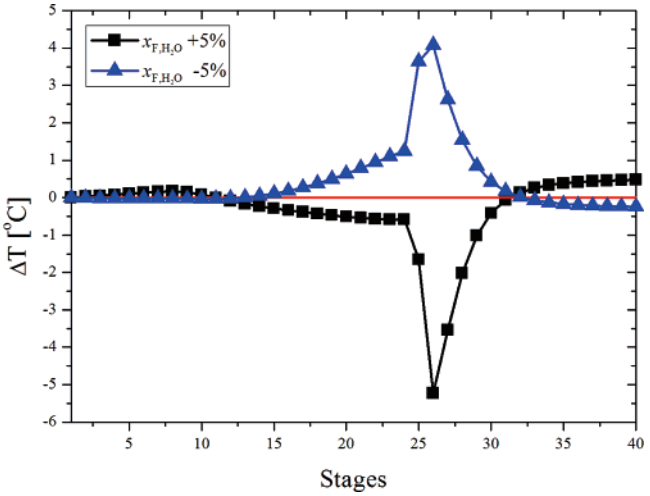

Figure 11. Closed-loop sensitivity plot for the disturbances of ±5% feedwater composition changes.

temperature control. From Table 1, it is found that both aqueous reflux flow rate and reboiler duty need to be adjusted to cope with the various feed disturbances. As a result, it is not possible to achieve the dual composition control with only a single temperature control loop.

Because the operating point is open-loop unstable, thus open-loop sensitivity analysis cannot be applied to determine the temperature control points. Instead, the closed-loop sensitivity analysis as in Lee et al.[13] is performed and shown in Figure 11. With ±5% changes in the feedwater composition, the temperature profiles under two perfect composition control loops are compared with the temperature profile of the base case. The two temperature control points should be chosen at the stages that have least deviation of the tray temperatures leaving the

Table 1. Values of the Two Manipulated Variables under Two Composition Controls ($x_{B,HAc}$ = 99.9 mol % and $x_{D,HAc}$ = 0.1 mol %)

composn control	aq reflux flow (mol/h)	reboiler duty (kW)
nominal condition	20.4567 (deviation %)	1393.4810 (deviation %)
x_{F,H_2O} +5%	22.8367 (11.63%)	1492.8027 (7.13%)
x_{F,H_2O} −5%	20.1386 (−1.55%)	1336.3404 (−4.10%)
$x_{F,PX}$ +10%	20.9546 (2.43%)	1403.7999 (0.74%)
$x_{F,PX}$ −10%	20.1192 (−1.65%)	1386.4798 (−0.50%)
ΔF +5%	21.4622 (4.92%)	1459.4518 (4.73%)
ΔF −5%	19.4494 (−4.92%)	1327.087 (−4.76%)
ΔF +10%	22.4689 (9.84%)	1525.056 (9.44%)
ΔF −10%	18.4360 (−9.88%)	1260.183 (−9.57%)

two product purity specifications (bottoms at 99.9 mol % HAc and top at 0.l mol % HAc) being met. On the basis of the results as shown in Figure 11, the temperature control points are selected at the 11th and 32nd stages (counting from column top to bottom). The final control strategy is then proposed as the one in Figure 12. Noticed that the other two operating variables (IBA makeup and sidedraw) not being used in the temperature control loops are all ratios to the fresh feed flow rate.

4.2. Closed-Loop Simulation Results. The closed-loop simulation results with ±5% feedwater composition disturbances are shown in Figure 13. The two product specifications are maintained quite nicely under these two unmeasured feed composition disturbances. For the disturbance with ±10% changes in the fresh feed flow rate, the set-points of the two temperature control loops need to be adjusted to maintain the product purities to meet their specifications. The reason for the necessary adjustments to the two set-points is because the pressures at the two temperature-controlled stages were changed along with the feed rate disturbances due to the varying of the pressure drop through each tray. The pressure drop through each

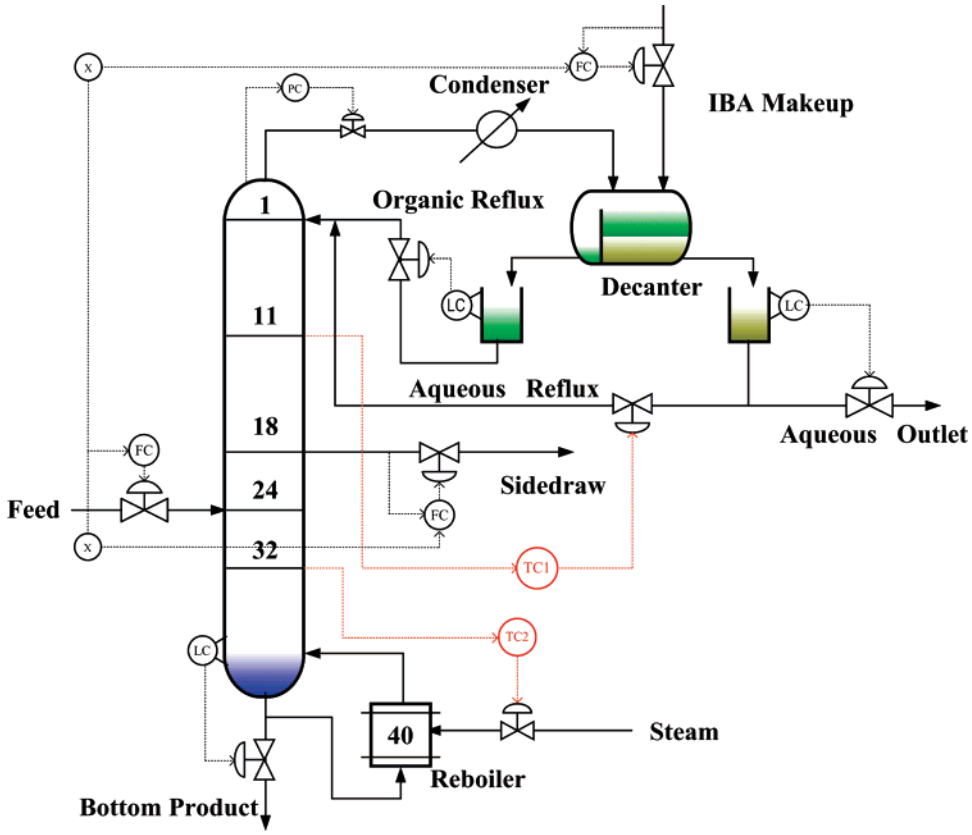

Figure 12. Proposed overall control strategy.

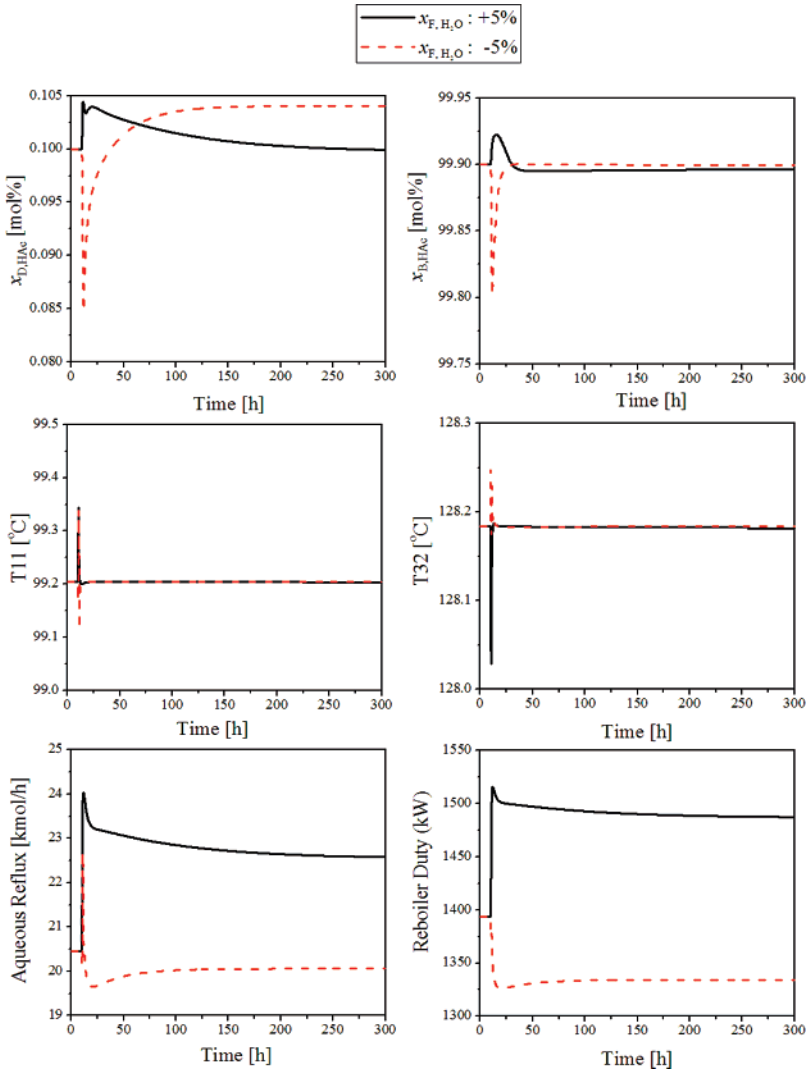

Figure 13. Closed-loop results for ±5% changes in the feedwater composition.

tray was determined by the liquid holdup at each tray and the vapor rate (influenced by the reboiler duty) through that tray, although the pressure at the top of the column is under controlled. Since the reboiler duty should be varied with the feed rate changes (see Table 1) to hold the two product specifications, the pressure at the temperature-controlled stages were changed accordingly. Because these fresh feed flow rate changes are considered as measurable disturbances, feedforward adjustments on the temperature set-point can be implemented. Figure 14 shows the values of the two temperature set-points under various fresh feed flow rates. From this figure, the set-points of the two temperature control loops can be determined to accommodate ±10% changes in the fresh feed flow rate. Figure 15 shows the closed-loop dynamic results with this feedforward control. Notice that, after implementation of this feedforward control, the two product purities meet successfully the high specification on purity.

The other feed composition disturbance considered is the changes in the feed PX composition. Figure 16 shows the closed-loop dynamic results with ±30% changes of PX composition. A +30% of PX composition change is equivalent to change of PX composition in the feed stream to 0.13 mol % together with the corresponding decrease of acetic acid. It is noticed that the two product purities deviated from their specifications, especially in the +30% case, where a largest deviation (bottoms product from 99.9 to 99.85 mol % HAc) occurs. Nevertheless, this deviation is considered acceptable because the purity is still very high.

Entirely different closed-loop dynamic results are obtained when changes of the feed PX composition are larger (±50% changes). Figure 17 shows the closed-loop results for these changes. One important observation is that the changes of the manipulated variables are not symmetric at all. Both manipulated variables need to be increased no matter if the changes of the feed PX composition are positive or negative. Especially, in the −50% case, both manipulated variables need to be at very high values. This causes much higher energy requirement and certainly is not desirable for only a small amount change in terms of composition of PX from 0.1 to 0.15 mol %.

The above asymmetric closed-loop behavior occurs even with two perfect composition control loops. With a gradually change of feed PX composition from base case to −90%, Figure 18 shows the temperature and composition profiles of the column with perfect control of two compositions. It is noticed that the behaviors of temperature and composition profiles gradually switch from one pattern to the other. For a change within −50% to −90% in PX composition, high-energy operation results which follows the path that has less or no PX in the bottom part of the column. This behavior was also noticed in the first

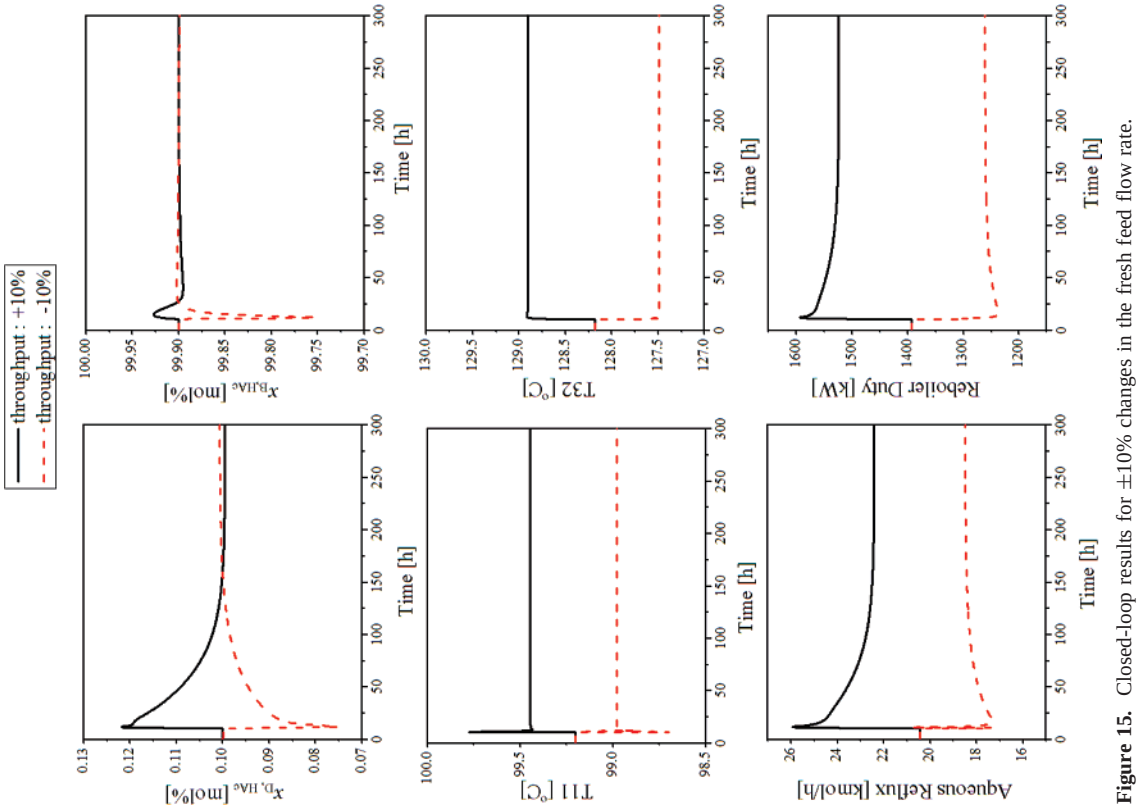

Figure 15. Closed-loop results for ±10% changes in the fresh feed flow rate.

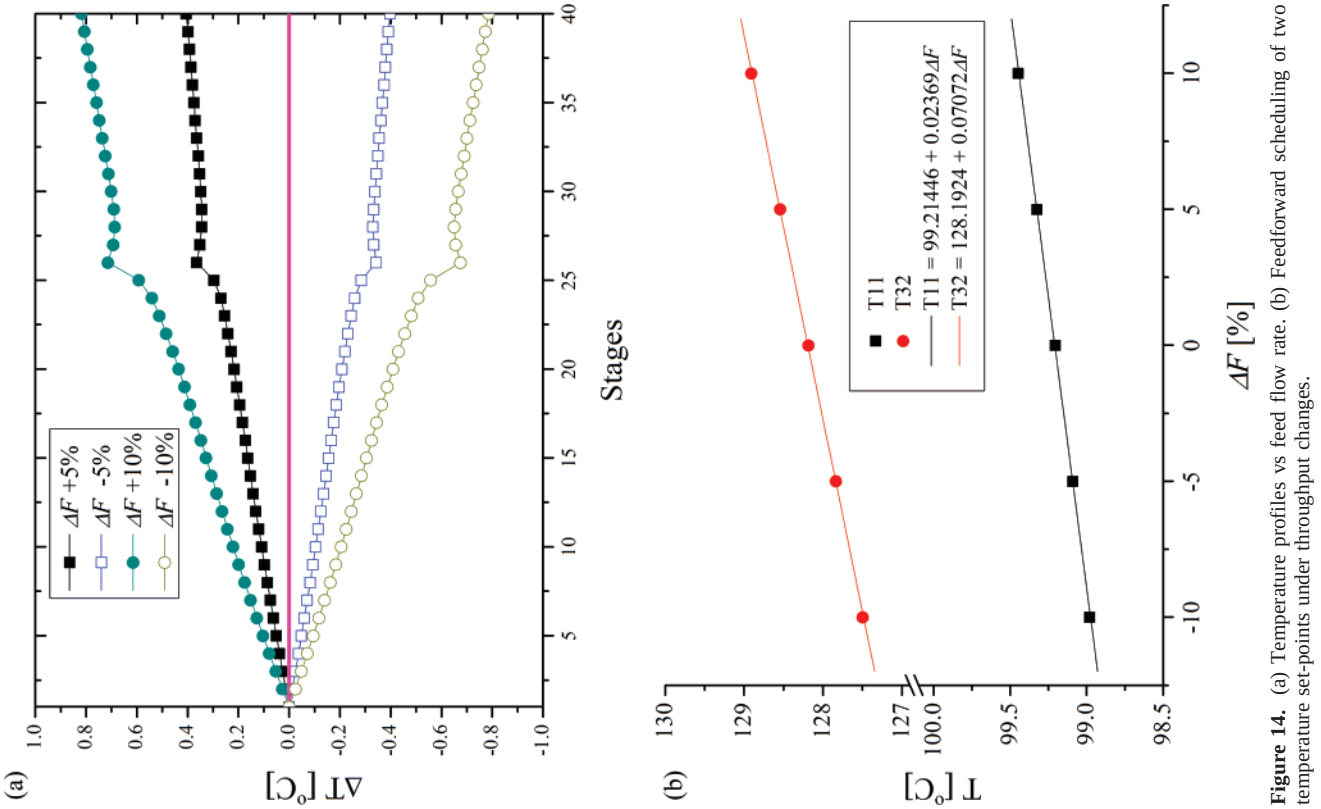

Figure 14. (a) Temperature profiles vs feed flow rate. (b) Feedforward scheduling of two temperature set-points under throughput changes.

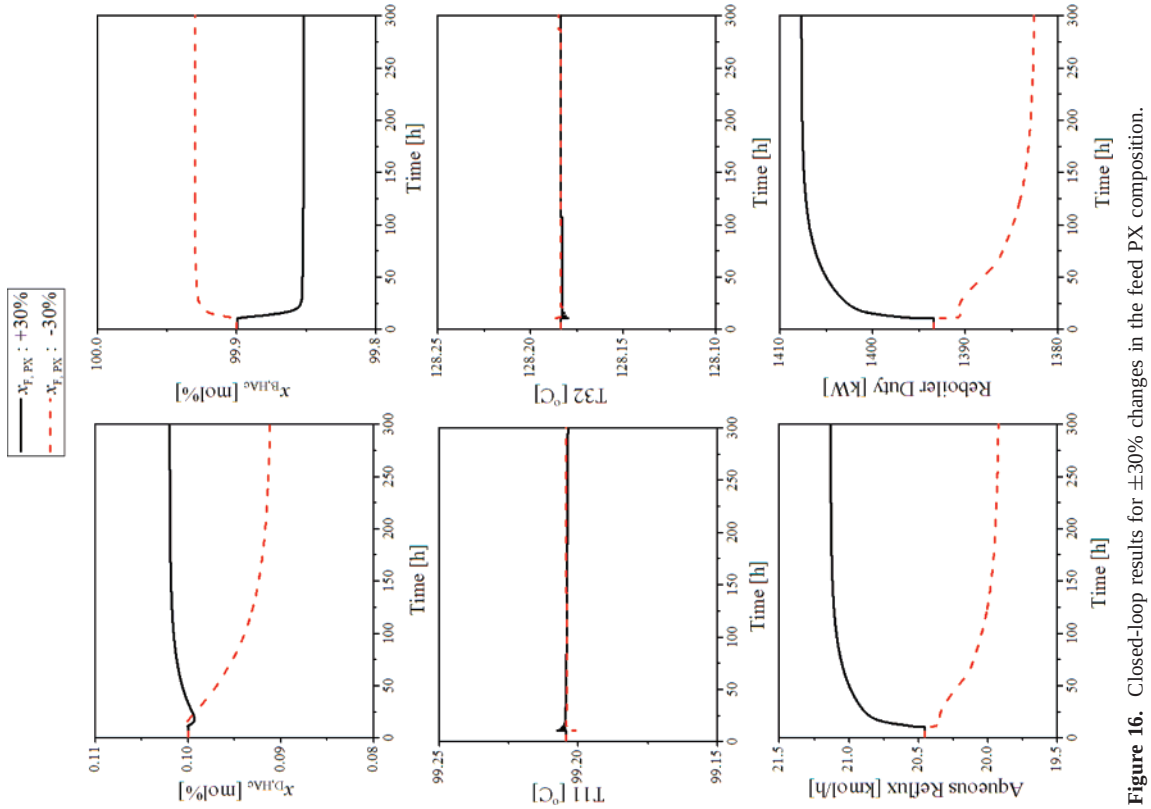

Figure 16. Closed-loop results for ±30% changes in the feed PX composition.

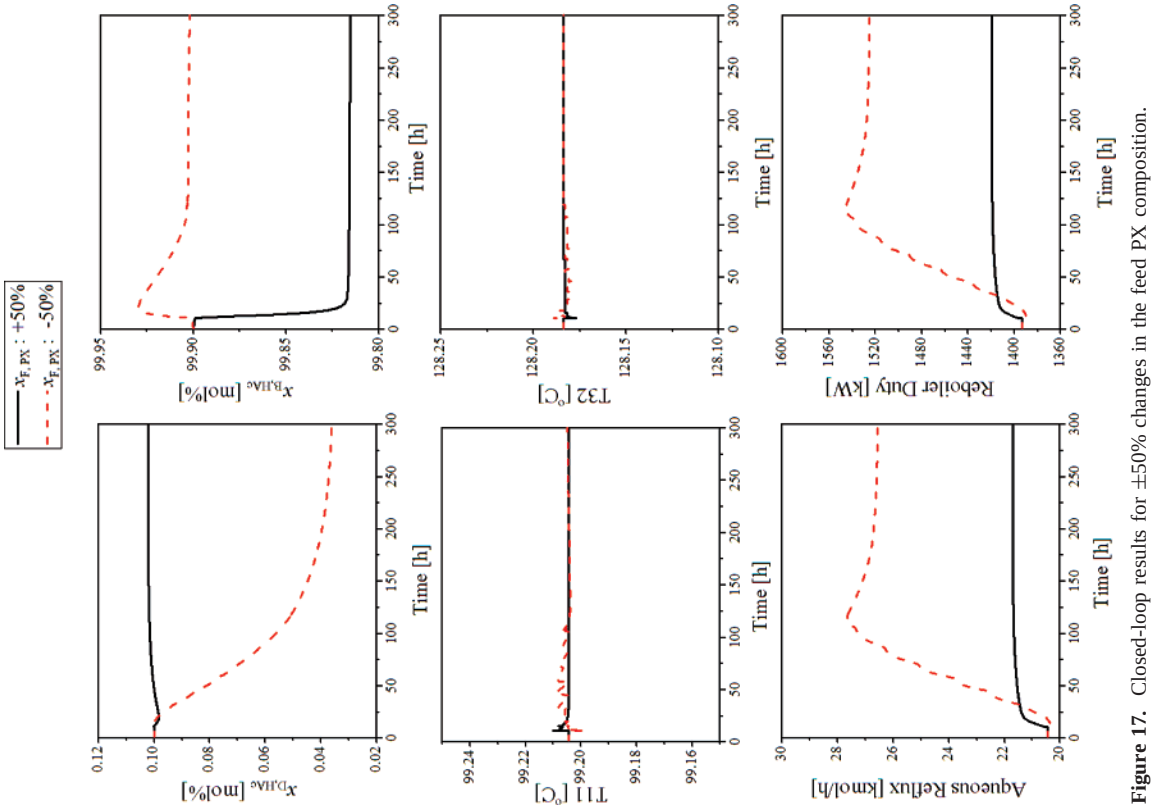

Figure 17. Closed-loop results for ±50% changes in the feed PX composition.

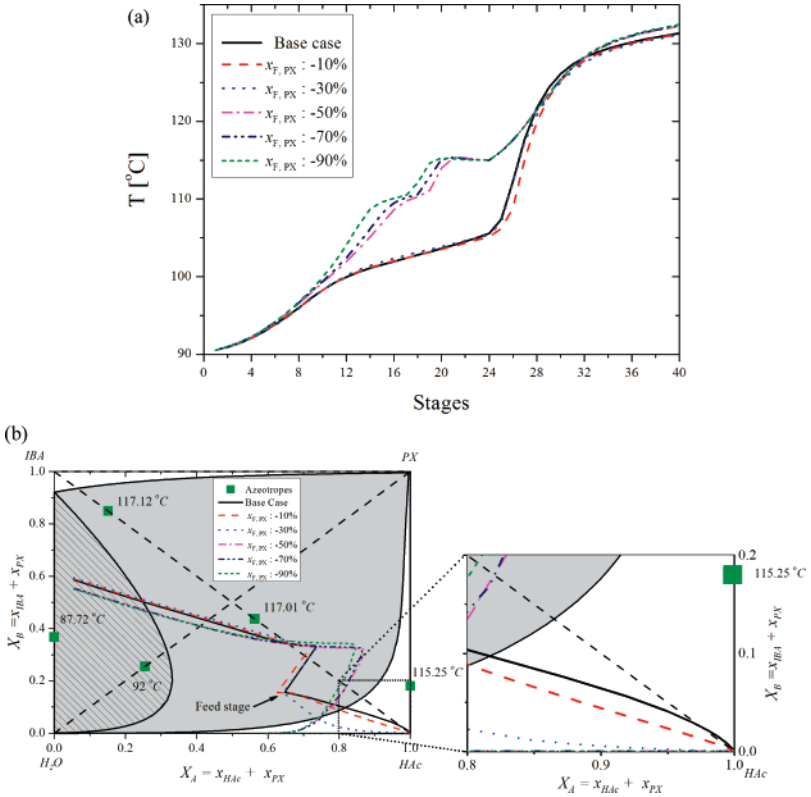

Figure 18. Temperature and composition profiles for various feed PX composition changes.

part of our paper, where, in the case when the feed tray location was not properly located, a high-energy operation resulted.

4.3. Side Stream Operating Strategy. An important conclusion that comes up with the above analysis is that it needs to keep proper PX concentration inside the column to ensure energy-efficient operation. For −50% to −90% changes in the feed PX composition, if the side streamflow rate is fixed constant, the PX will be depleting from the column and thus cause high-energy operation. This was certainly not the attention before, as we design the side stream to take PX out to prevent accumulation of PX inside the column. A side stream operating strategy thus needs to be devised to keep proper PX concentration inside the column subjected to disturbances from feed composition.

Since measuring composition especially inside the column is impractical in industry, we will use some tray temperature measurement as an indication for manipulating the side stream. Figure 19a shows the dynamic responses of the column temperature profile under dual-point temperature control (e.g., Figure 12) subjected to a PX composition change of −50%. It seems that temperature at stage 25 can be used as an indication to shut the side stream valve to preserve PX inside the column. However, as shown in Figure 19b, the temperature profile in response to another different disturbance (−5% feedwater composition change) has also a considerable increase of temperature on stage 25. Thus, a criterion to differentiate between these two types of unmeasured disturbances is desirable.

One of the differences between these two types of disturbances is that the increase of temperature has much faster rate when water composition changes than PX composition does. The dynamic characteristics of the two types of feed changes as well as the feed rate change are shown in Figure 20. For the PX composition changes (−50% to −90%), temperature at stage 25 has more than a 5 °C increase. On the other hand, smaller PX changes (e.g. −30%) do not have this large temperature variation. Assuming the biggest feed PX composition drop is −90%, a manipulating strategy is proposed as follows to differentiate the PX change from the feedwater change.

In the figure, t_1 is defined as the starting time when the temperature at stage 25 departs from its nominal temperature. A noise band can be defined for the possible noisy measurement of this stage temperature. Also in the figure, t_2 is defined as the stop time when the temperature difference is at 5 °C. If $t_2 - t_1$ is greater than 2 h, which means that this is not feedwater composition disturbance, than the side stream valve is closed to preserve PX inside the column. When temperature at stage 25 is back to 108 °C, the side stream valve is opened back to resume its nominal flow rate.

Figure 21 shows the closed-loop result of the dual-point temperature control together with this side stream operating strategy, when −50% feed PX composition disturbance is introduced at a time of 10 h and then back to original feed composition at a time of 300 h. It is found that both products are maintained at high purity and, more importantly, the aqueous reflux flow rate and reboiler duty are kept at low values (comparing to the results in Figure 17). Figure 22 shows the dynamic responses of the side streamflow rate and the column temperature profile. It is noticed that the side stream valve is periodically closed between 10 and 300 h to preserve PX in the column. After a time at 300 h, the side streamflow rate is desirably returning back to its nominal value following the proposed side stream operating strategy.

Figures 23 and 24 show plots similar to those in Figures 21 and 22 but with a −90% feed PX composition disturbance. The two products are still maintained at high purity with low aqueous reflux flow rate and reboiler duty. During the time period under a −90% feed PX composition disturbance, the side stream valve is closed accordingly to preserve PX concentration in the

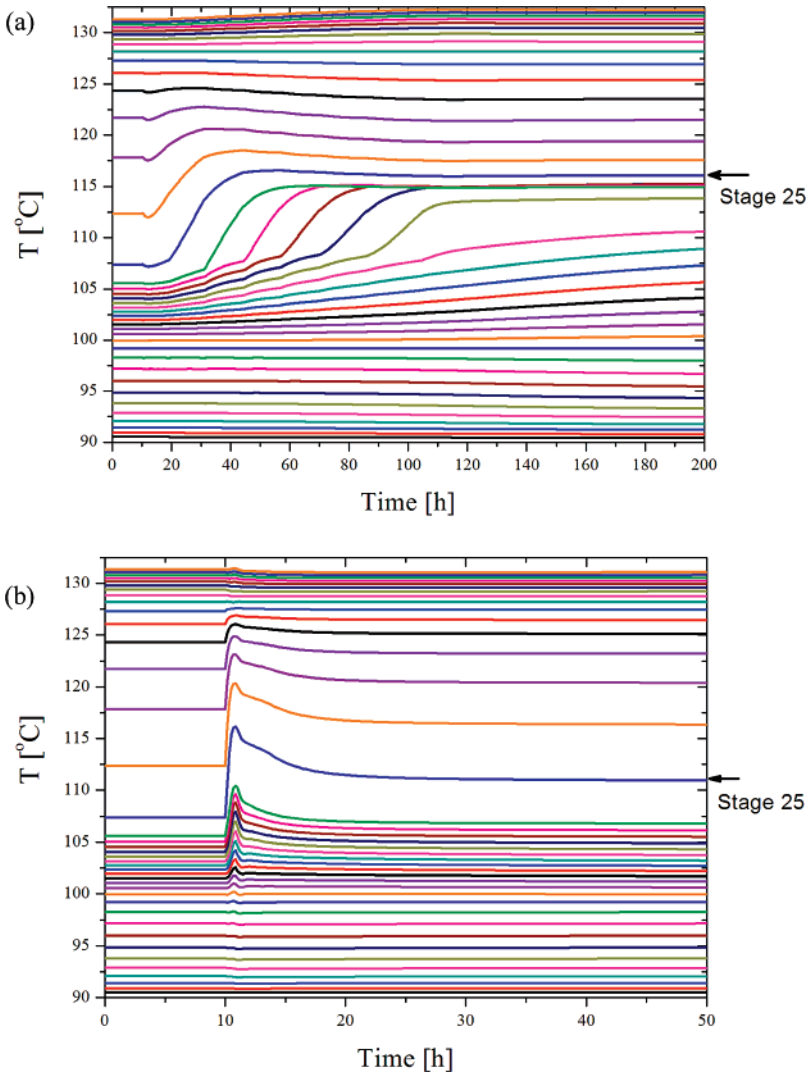

Figure 19. Dynamic responses of stage temperatures: (a) −50% change in feed PX composition; (b) −5% change in feedwater composition.

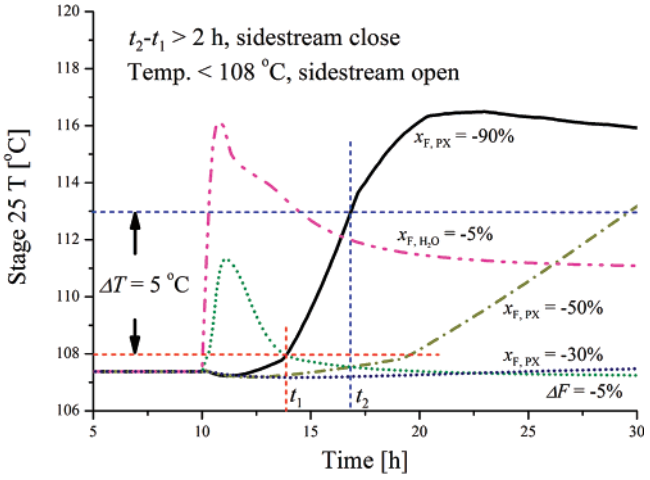

Figure 20. Dynamic response of stage 25 temperature under various disturbances.

column. Comparing the results in Figure 24 to those of Figure 22, it is noticed that closing of side stream valve is more frequent for this −90% feed PX composition disturbance. This makes sense because that less PX than the previous case goes into the column. When feed composition is returning back to normal at a time of 300 h, the proposed side stream operating strategy brings the side streamflow rate back to its nominal value as expected.

5. Conclusion

In summary, there are several important findings from this study: (1) The bifurcation phenomenon was found in the case of feed with impurity no matter whether the column has a side stream or not. However, this phenomenon was not found for the case of feed without impurity. (2) For the case of feed with impurity, the column should be operated at an operating point which is open-loop unstable. If operating at a stable steady state is desired, 10% more reboiler duty is needed for lower purity case and much greater reboiler duty is needed for higher purity case. (3) Dual-point temperature control strategy is needed for the case of feed with impurity. On the contrary, as seen in Chien et al.,[10] only single-point strategy is required for the case of feed without impurity. (4) PX concentration inside the column needs to be maintained to keep the composition profile following the path with more PX in the bottom part of the column. To ensure energy-efficient operation of the column, a side stream operating strategy is devised to preserve PX inside the column. (5) The proposed overall control strategy is tested under various feed disturbances. High-purity products (column bottoms and top) can still be obtained despite disturbances.

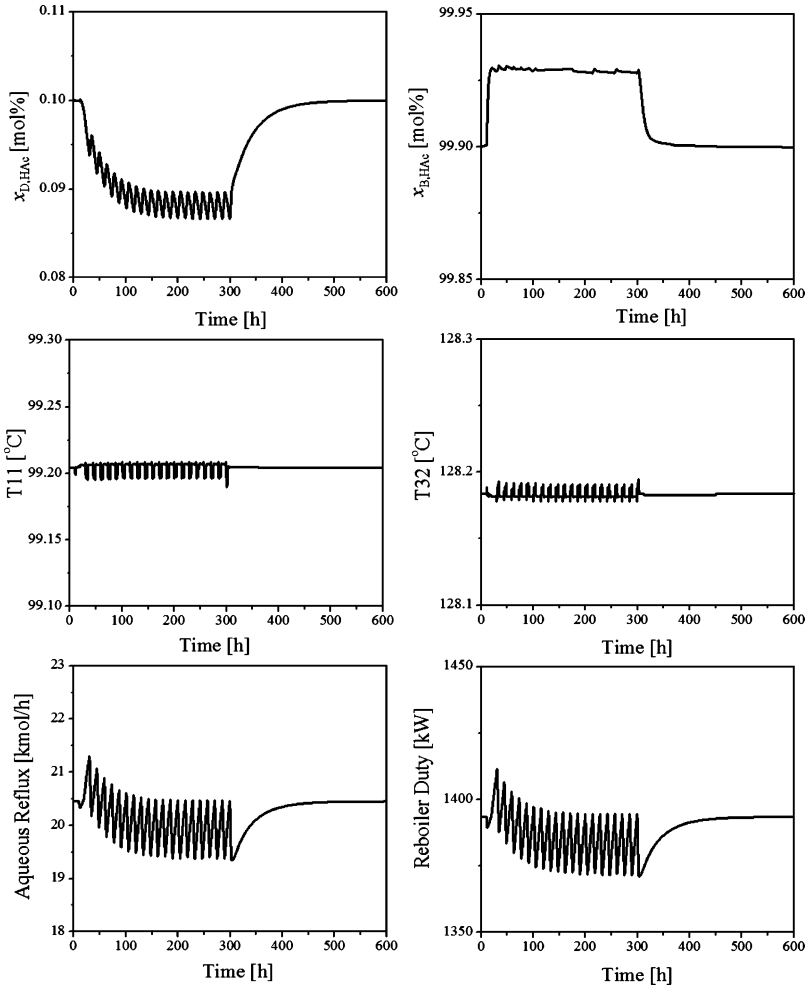

Figure 21. Closed-loop results with side stream operating strategy (time = 10 h, from nominal condition to −50% changes in the feed PX composition; time = 300 h, from −50% changes in the feed PX composition to nominal condition).

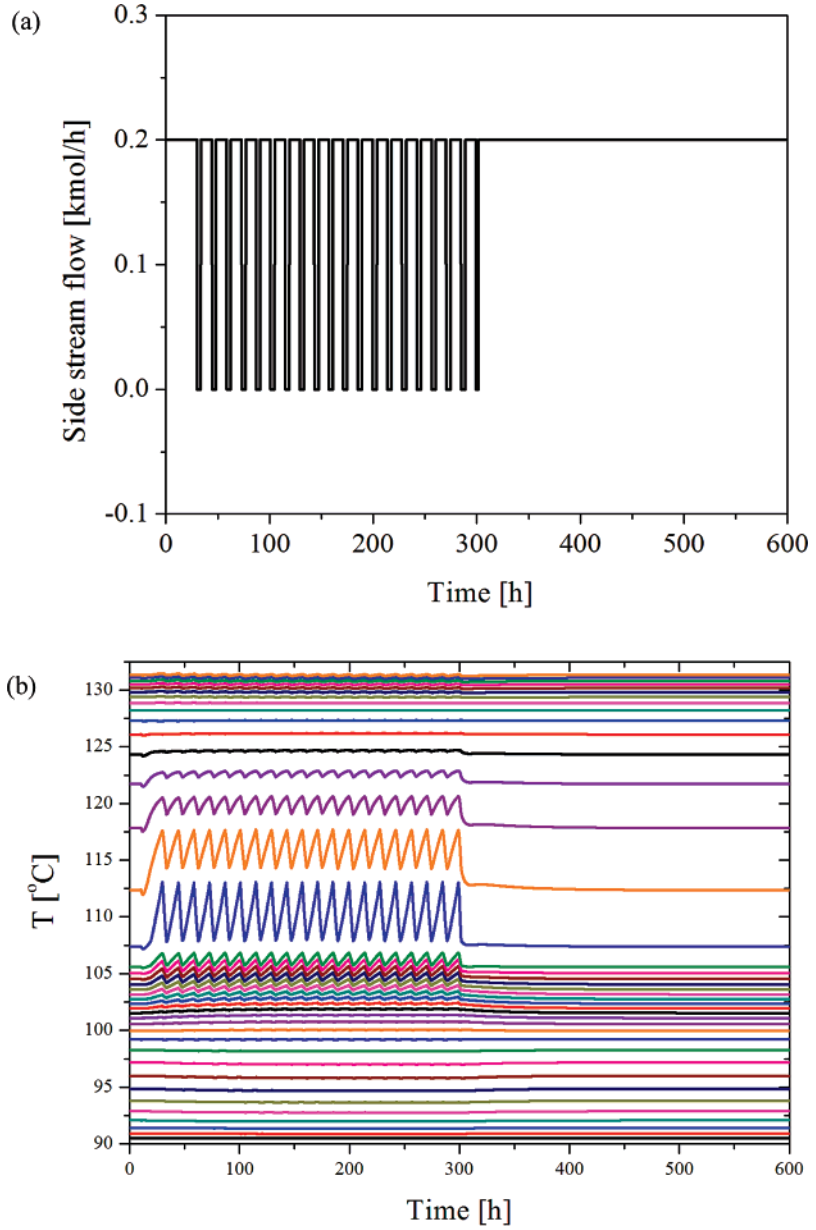

Figure 22. Side streamflow rate and tray temperatures with side stream operating strategy for the above disturbance changes shown in Figure 21.

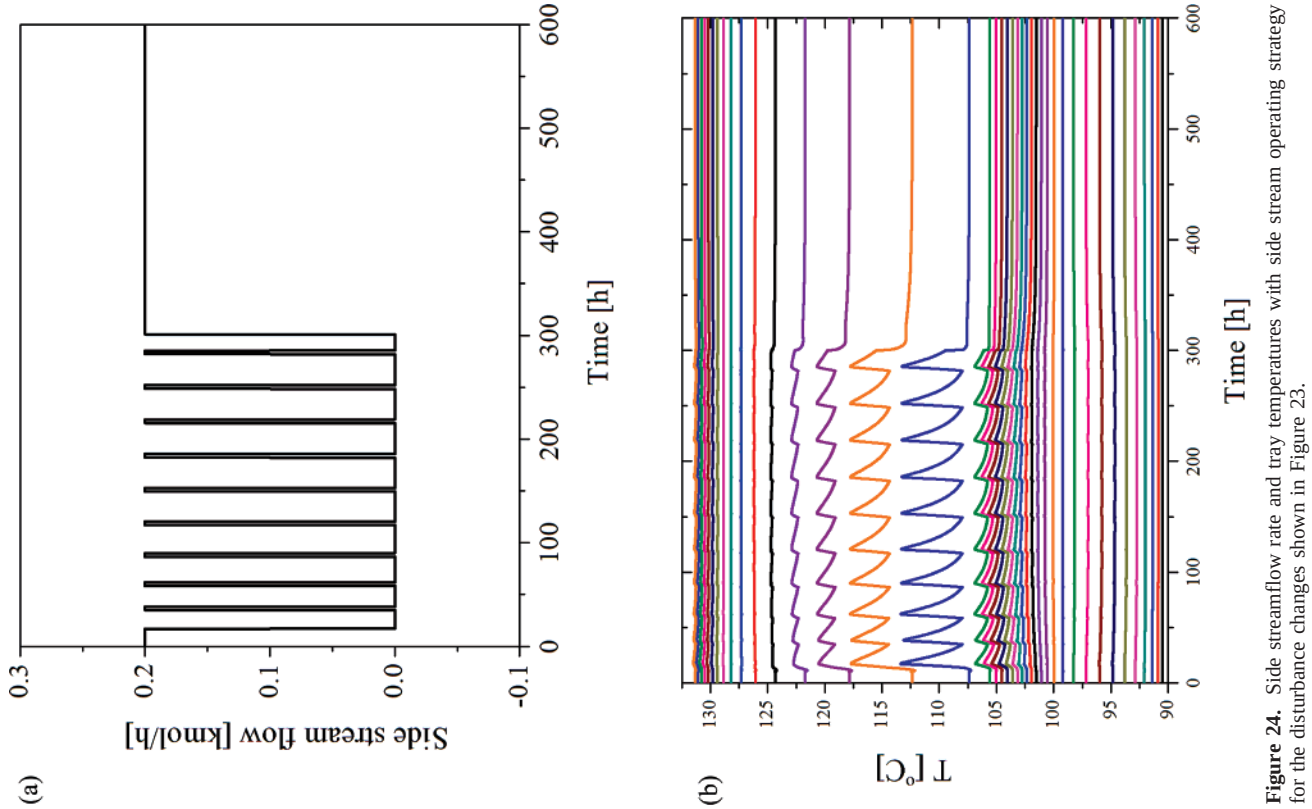

Figure 24. Side streamflow rate and tray temperatures with side stream operating strategy for the disturbance changes shown in Figure 23.

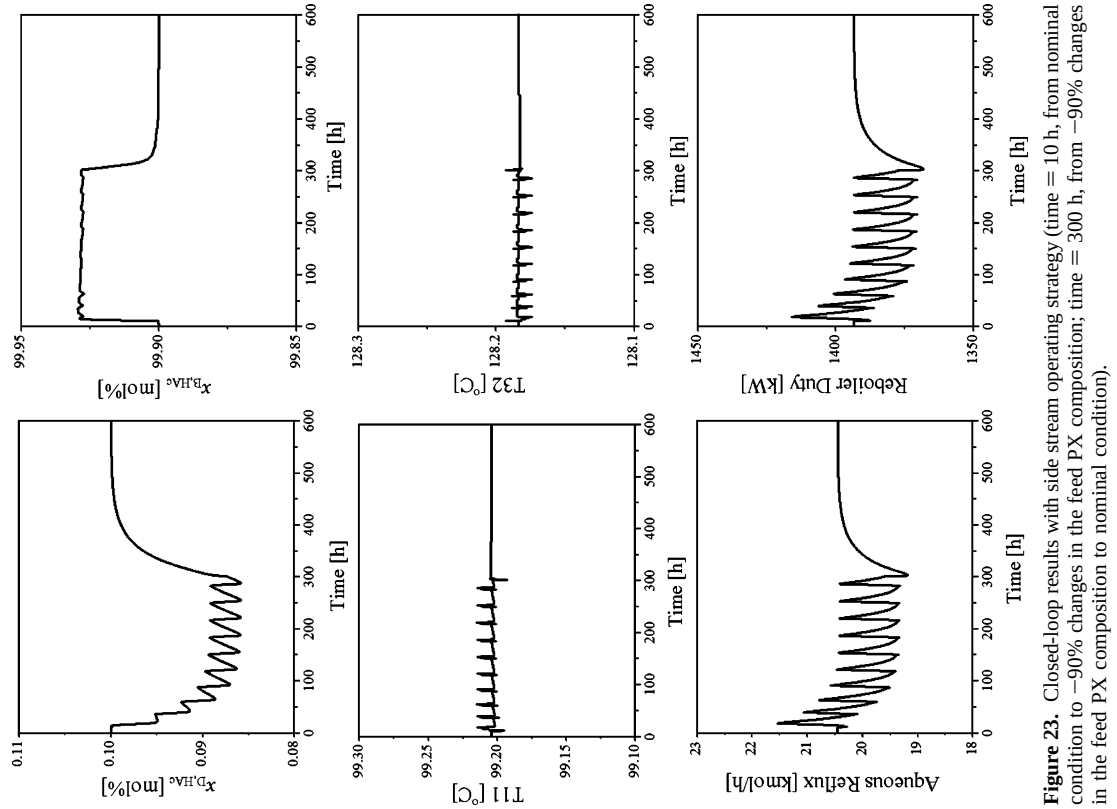

Figure 23. Closed-loop results with side stream operating strategy (time = 10 h, from nominal condition to −90% changes in the feed PX composition; time = 300 h, from −90% changes in the feed PX composition to nominal condition).

Acknowledgment

This work is supported by the Ministry of Economic Affairs of the ROC under Grant No. 95-EC-17-A-09-S1-019.

Literature Cited

(1) Huang, H. P.; Lee, H. Y.; Gau, T. K.; Chien, I. L. Design and Control of Acetic Acid Dehydration Column with *p*-Xylene or *m*-Xylene Feed Impurity. 1. Importance of Feed Tray Location on the Process Design. *Ind. Eng. Chem. Res.* **2007**, *46*, 505−517.

(2) Hindmarsh, E.; Turner, J. A.; Ure, A. M. Process for the production of terephthalic acid. U.S. Patent 5563293, Oct 8, 1996.

(3) Lee, F. M.; Lamshing, W.; Wytcherley, R. W. Method and Apparatus for Preparing Purified Terephthalic Acid and Isophthalic Acid from Mixed xylenes. U.S. Patent 6054610, April 25, 2000.

(4) Othmer, D. F. Azeotropic Separation. *Chem. Eng. Prog.* **1963**, *59* (6), 67−78.

(5) Pham, H. N.; Doherty, M. F. Design and Synthesis of Heterogeneous Azeotropic Distillations-III. Column Sequences. *Chem. Eng. Sci.* **1990**, *45* (7), 1845−1854.

(6) Tanake, S.; Yamada, J. Graphical Calculation Method for Minimum Reflux Ratio in Azeotropic Distillation. *J. Chem. Eng. Jpn.* **1972**, *5*, 20−26.

(7) Othmer, D. F. Azeotropic Distillation for Dehydrating Acetic Acid. *Chem. Metall. Eng.* **1941**, *40*, 91−95.

(8) Siirola, J. J. An Industrial Perspective on Process Synthesis. In *AIChE Symposium Series No. 304*; Biegler, L. T., Doherty, M. F., Eds.; CACHE: Austin, TX, 1995; Vol. 91, pp 222−233.

(9) Wasylkiewicz, S. K.; Kobylka, L. C.; Castillo, F. J. L. Optimal Design of Complex Azeotropic Distillation Columns. *Chem. Eng. J.* **2000**, *79*, 219−227.

(10) Chien, I. L.; Zeng, K. L.; Chao, H. Y.; Liu, J. H. Design and Control of Acetic Acid Dehydration System via Heterogeneous Azeotropic Distillation. *Chem. Eng. Sci.* **2004**, *59* (21), 4547−4567.

(11) Chien, I. L.; Huang, H. P.; Gau, T. K.; Wang, C. H. Influence of Feed Impurity on the Design and Operation of an Industrial Acetic Acid Dehydration Column. *Ind. Eng. Chem. Res.* **2005**, *44*, 3510−3521.

(12) Cruickshank, A. J. B.; Haertsch, N.; Hunter, T. G. Liquid−Liquid Equilibrium of Four-Component Systems. *Ind. Eng. Chem.* **1950**, *42*, 2154.

(13) Lee, H. Y.; Huang, H. P.; Chien, I. L. Control of Reactive Distillation Process for Production of Ethyl Acetate. *J. Process Control* **2007**, *17*, 363.

Received for review July 4, 2007
Revised manuscript received February 19, 2008
Accepted February 20, 2008

IE070916F